Methane escape from Titan's atmosphere

R. V. Yelle,[1] J. Cui,[1] and I. C. F. Müller-Wodarg[2]

[1]   Measurements of the mole fractions of CH_4 and ^{40}Ar by the Ion Neutral Mass Spectrometer on the Cassini orbiter are analyzed to determine the rate of vertical mixing in Titan's atmosphere and the escape flux of CH_4. Analysis of the ^{40}Ar data indicates an eddy mixing rate of $2–5 \times 10^7$ cm^2 s^{-1}, an order of magnitude smaller than previously determined from analysis of the CH_4 distribution. The eddy profile determined from the ^{40}Ar data implies that CH_4 distribution is best explained by postulating that it is escaping the atmosphere at the diffusion limited rate of $2.5–3.0 \times 10^9$ cm^{-2} s^{-1}, referred to the surface. This represents a significant loss of atmospheric CH_4, smaller than but comparable to the photochemical destruction rate. The escape rate is much larger than predicted by the Jeans escape formula and vigorous nonthermal mechanisms are not apparent.

1.   Introduction

[2]   The CH_4 distribution in Titan's upper atmosphere remains uniformly mixed until ~1100 km, where it begins to exhibit diffusive separation. This characteristic was first seen in analysis of the Voyager UVS occultation measurements [*Smith et al.*, 1982; *Strobel et al.*, 1992; *Vervack et al.*, 2004] and has been verified recently by in situ measurements from the Cassini Ion Neutral Mass Spectrometer (INMS) [*Yelle et al.*, 2006]. The CH_4 profile was originally interpreted as a consequence of large eddy mixing rates that implied a homopause, the boundary between the well-mixed and diffusively separated regions of the atmosphere, at high altitude; however, *Yelle et al.* [2006] have pointed out that the CH_4 observations could be explained equally well by postulating a large escape flux. With only CH_4 data, it is impossible to decide between these two possibilities. The eddy diffusion coefficient required to explain the CH_4 distribution in the absence of escape is quite large, on the order of a few times 10^8 m^{-2} s^{-1}, which is 1–2 orders of magnitude larger than the eddy coefficients at the homopause in other atmospheres. The large eddy mixing hypothesis was the only one considered previously because rapid escape of CH_4 was considered unlikely. The Jean's escape flux of CH_4 from Titan is negligible and vigorous nonthermal escape mechanisms are not apparent.

[3]   The ambiguity in the interpretation of the CH_4 altitude profile is a consequence of the fact that the distribution of light species is affected by both a vertical flux and eddy mixing. An upward flux causes the density profile of a light species to remain parallel to that of the ambient atmosphere despite the tendency for diffusive separation to cause an increase with altitude. However, vertical mixing of the atmosphere, commonly parameterized in terms of an eddy diffusion coefficient, has a similar effect. The flux of a minor constituent can be expressed as

$$\Phi_i = -(D_i + K)N_a \frac{dX_i}{dr} - D_i N_a \left(\frac{1}{H_i} - \frac{1}{H_a} \right) X_i \qquad (1)$$

where Φ_i and X_i are the flux and mole fraction of the ith constituent, D_i is the molecular diffusion coefficient, K is the eddy diffusion coefficient, H_i and H_a are the diffusive equilibrium scale heights of the ith constituent and the background atmosphere, and N_a is the number density of the atmosphere. Solving equation (1) for dX_i/dr, we have

$$\frac{dX_i}{dr} = \frac{D_i}{D_i + K} \left(\frac{1}{H_a} - \frac{1}{H_i} \right) \left(1 - \frac{\Phi_i}{\Phi_l} \right) \qquad (2)$$

where Φ_l is the diffusion-limited flux defined by

$$\Phi_l = D_i N_a \left(\frac{1}{H_a} - \frac{1}{H_i} \right) X_i \qquad (3)$$

Φ_l is a physical limit on the magnitude of the upward flux because fluxes larger than Φ_l imply negative mole fractions near the top of the atmosphere [*Hunten*, 1973a, 1973b]. Equation (2) shows that dX_i/dr becomes small when $K/D \gg 1$ or when $\Phi_i \simeq \Phi_l$. Thus, a large escape flux has the same effect as a large eddy coefficient, both drive the altitude profile of a minor species toward a constant mole fraction. *Yelle et al.* [2006] have shown that the altitude profile of CH_4 measured by the Ion Neutral Mass Spectrometer (INMS) on the Cassini spacecraft during the first Titan encounter (TA) could be fit with models that had either a large eddy coefficient or a large escape rate and presented the combinations of eddy diffusion coefficient and escape flux that matched the observations.

[1]Department of Planetary Sciences, University of Arizona, Tucson, Arizona, USA.
[2]Space and Atmospheric Physics Group, Imperial College London, London, UK.
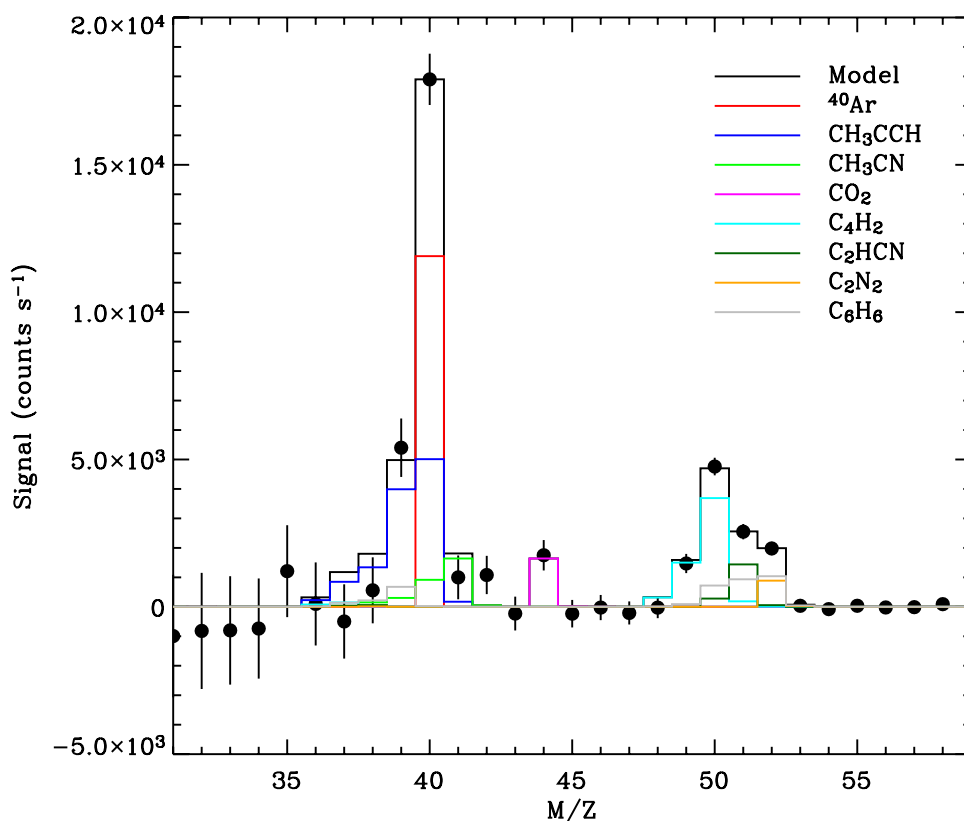
Figure 1. The mass spectrum of Titan's neutral atmosphere in the 950–1000 km region from the T16 pass. The data points represent the INMS measurements, and the black line represents a model fit to the spectrum. The colored lines show the contribution of various species to the spectrum.

[4] The ambiguity between the escape flux and eddy mixing explanations can be broken through examination of other tracers of atmospheric transport. Here, we analyze the altitude profiles of ^{40}Ar, in order to independently determine the eddy diffusion coefficient and thereby determine the CH_4 escape rate. We find that the eddy diffusion coefficient on Titan is lower than previously thought and that CH_4 is escaping at close to the diffusion-limited rate. The escape rate is only slightly smaller than the photochemical destruction rate of CH_4 and therefore must also play a role in the evolution of Titan's atmosphere.

2. Data Analysis

[5] In the standard operating mode, INMS measures count rates from mass-to-charge values (M/Z) of 1–8 and 12–99 sequentially sampling at approximately 30 Hz. These data can be examined in two complementary ways. We can collect the counting rate as a function of M/Z over a significant altitude range thereby constructing a spectrum of count rate versus M/Z, or we can examine the counts at a specific M/Z as a function of time or the associated altitude. The former approach is better for precise determination of the relative densities averaged over a large altitude range and is required for analysis of complex regions of the spectrum. The latter approach is preferable for examination of altitude profiles and works well in regions of the spectrum for which the confusion of cracking patterns is not too great. We will examine the ^{40}Ar distribution with

the altitude profile technique, but first we examine a typical spectrum.

[6] Figure 1 shows an INMS spectrum accumulated on the inbound pass for T16 at altitudes between 950 and 1000 km. The peak at M/Z = 40 is due primarily to ^{40}Ar, though several species contribute to the count rates in this mass range. Also, shown in Figure 1 is a fit to the spectrum based on the optimum densities for a suite of constituents determined by a singular value decomposition fit to the data [*Cui et al.*, 2008]. We use the results of the spectral analysis to devise an algorithm to derive the densities directly from the count rates in the relevant channels. The counts in M/Z = 40 are due to ^{40}Ar, CH_3CCH, and CH_3CN. The CH_3CN density is determined from the count rate in channel M/Z = 41, where it contributes essentially all the signal. The density of CH_3CCH is determined from the count rate in channel M/Z = 39, after the contributions of CH_3CN and C_6H_6 have been subtracted. The density of C_6H_6 is determined from the count rates in M/Z = 74–78 (not shown), where it is the only significant contributing species [*Vuitton et al.*, 2008]. The measurements in these other channels are not made simultaneously with the M/Z = 40 measurements and it is necessary to interpolate all measurements to a common time base. However, since the measurements are nearly sequential in M/Z, the interpolations are usually within 100 ms of the M/Z = 40 measurement. We thus estimate the ^{40}Ar density for each M/Z = 40 measurement. Comparison of the results from the spectral analysis with the values from the point-by-point analysis averaged over the
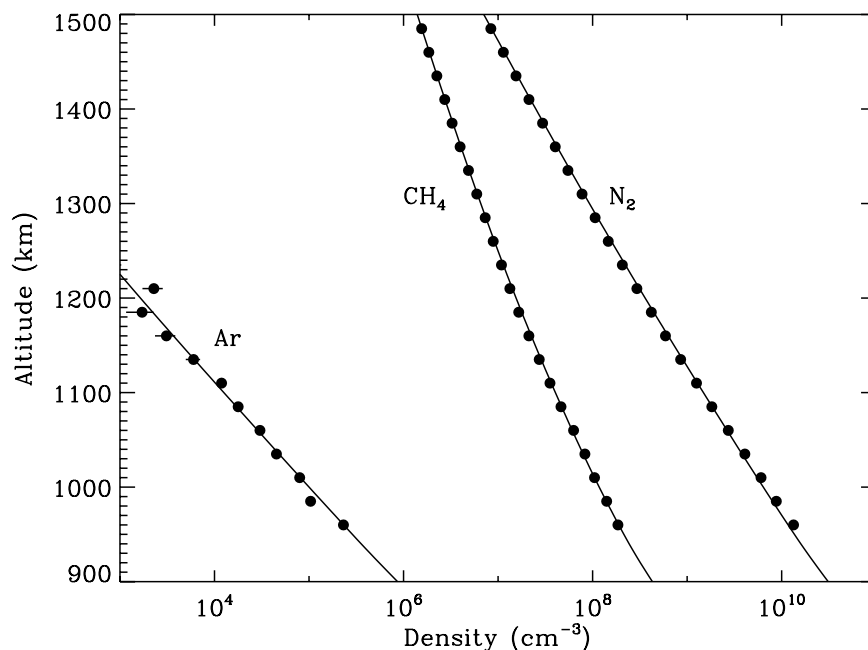
Figure 2. The average N_2, CH_4, and ^{40}Ar densities measured by the INMS on the inbound legs of Cassini Titan flybys. Error bars are based on counting statistics and do not include calibration uncertainties or latitudinal variations. For N_2 and CH_4 the error bars are smaller than the plot symbols. The solid curve intersecting the ^{40}Ar data represent diffusion models discussed further in the text. The solid curves intersecting the N_2 and CH_4 data represent the empirical model of *Müller-Wodarg et al.* [2008] for 60°N latitude.

same altitude range indicate that the two methods agree to within 10%.

[7] The N_2 and CH_4 densities are determined from INMS measurements in a similar manner, though fewer channels are required and other corrections come into play. A full description of the method used for those constituents is given by *Müller-Wodarg et al.* [2008] and *Yelle et al.* [2006].

[8] Measurements of neutral constituent densities have been made during multiple passes of the Cassini spacecraft through Titan's upper atmosphere at various latitudes, local times, and longitudes [*Waite et al.*, 2007; *Müller-Wodarg et al.*, 2008]. The altitude distribution of even inert chemical constituents may vary horizontally because of the interplay of advection and diffusive separation [*Müller-Wodarg and Yelle*, 2002]. Nevertheless, we will analyze the average CH_4 and ^{40}Ar profiles with a 1D model in order to determine the eddy diffusion coefficient and CH_4 escape rate. There are two reasons for this choice. First, because of its low abundance, the ^{40}Ar data to be analyzed here are characterized by a low signal-to-noise ratio (SNR) in a single pass and better constraints are obtained by averaging multiple passes to increase SNR. Second, analysis in terms of an eddy diffusion coefficient is most relevant for large horizontal averages that smooth out dynamical effects. Redistribution of constituents by dynamics is an interesting question, but here our focus is on the eddy coefficient and CH_4 escape rate and averaging over horizontal variations is beneficial. A similar approach in a study of the H_2 distribution and escape rate is used in the work of *Cui et al.* [2008]. As discussed in the work of *Müller-Wodarg et al.* [2008], Cassini low-altitude passes for which the INMS has made measurements are concentrated in Titan's northern hemisphere. Our results therefore pertain to northern midlatitudes. The geometrical information for the individual Titan passes is summarized by *Müller-Wodarg et al.* [2008].

[9] The average profiles for N_2, CH_4, and ^{40}Ar are constructed from the profiles for individual passes by first resampling all profiles to a common altitude grid followed by simple averaging. Figure 2 shows the ^{40}Ar, CH_4 and N_2 densities versus altitude determined with the technique described above. Error bars reflect the uncertainty due to counting statistics. The uncertainty in absolute calibration of ~20% [*Waite et al.*, 2004] (not included in the figures) affects the density curves for the different species relative to each other, but does not affect the shape of the altitude profile for a particular molecule. The altitude profiles show that N_2, CH_4, and ^{40}Ar are characterized by different scale heights, revealing the importance of diffusive separation in this region of the atmosphere. The solid curves passing through the N_2 and CH_4 data in Figure 2 are results from the empirical model of *Müller-Wodarg et al.* [2008] evaluated at a latitude of 60°N. The agreement with the average N_2 and CH_4 computed here is better than 2% at all but the highest altitudes. The solid curve passing through the ^{40}Ar data points is the result of a diffusion calculation to be described in more detail below. Here, we simply note that the altitude distribution of ^{40}Ar is characterized by a scale height for a species of mass 40, indicating that this altitude range is above the ^{40}Ar homopause.

[10] The temperature profile above 1000 km is well determined by INMS measurements [*Müller-Wodarg et al.*, 2008], but in section 3 we show that diffusive separation for ^{40}Ar on Titan begins at about 800 km. This is below the lowest altitudes sampled by the INMS and, in fact, inference
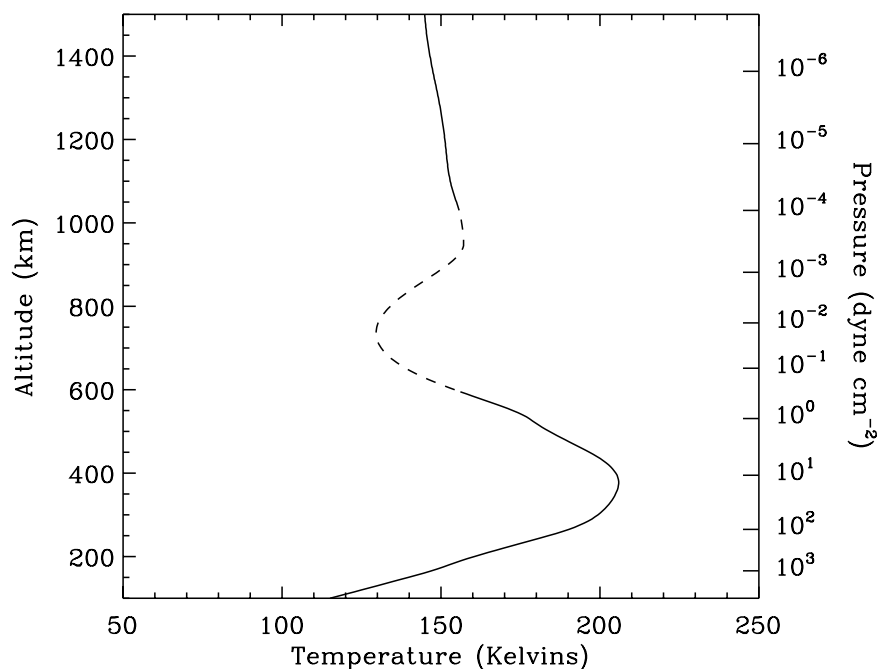
Figure 3. Temperature profiles for Titan's atmosphere. Below 500 km we use the results of *Vinatier et al.* [2007] for 56°N latitude, based on Cassini/CIRS spectral measurements. Above 1000 km we use the empirical model of *Müller-Wodarg et al.* [2008] for 60°N latitude, which is based on Cassini/INMS measurements. In the region from 500 to 1000 km we use an interpolation that satisfies the hydrostatic equilibrium constraint.

of pressures and temperatures in this region (sometimes called the ignorosphere, or more recently the agnostosphere) are difficult to come by. However, we need an estimate of the atmospheric structure in order to model diffusive separation. Temperatures in the stratosphere and mesosphere up to altitudes of ∼500 km have been inferred by limb scans of CH_4 thermal emissions by the Cassini Composite Infrared Spectrometer (CIRS) [*Vinatier et al.*, 2007]. To construct a complete temperature profile we interpolate between the INMS results and CIRS results at a latitude of 56°N using a fifth degree polynomial for temperature versus altitude. Results are shown in Figure 3. The interpolation matches the magnitude and slope of temperature at the upper and lower boundaries and satisfies the hydrostatic equilibrium constraints between these two levels, providing 5 constraints that uniquely determine the 5 polynomial coefficients. The mean molecular mass of the atmosphere as a function of altitude is required for the hydrostatic equilibrium calculations and is obtained from the diffusion models discussed below. The derived temperature profile differs significantly from those deduced by *Shemansky et al.* [2005], but that work is in conflict with INMS measurements.

3. Vertical Mixing Rate and CH_4 Escape Flux

[11] We model the altitude profiles of N_2, CH_4 and ^{40}Ar by solving the coupled vertical diffusion equations and continuity equations along with the equation for hydrostatic equilibrium, taking into account the effect of diffusive separation on the mean molecular mass of the atmosphere. The calculations extend from 100 km to 1500 km with 5 km

resolution and utilize the temperature profile presented in section 2. Diffusion coefficients are taken from *Mason and Marrero* [1970]. Spherical coordinates are used for the expression of flux divergence and the variation of gravity with distance from Titan's center is included. The mole fractions of N_2, CH_4, and ^{40}Ar are fixed at the lower boundary while fluxes are specified at the upper boundary. In all cases we assume that the fluxes of N_2 and ^{40}Ar are zero, but find that we must include a significant CH_4 flux to obtain an adequate match to the data. The eddy diffusion coefficient, $K(z)$ is the only additional free parameter in the calculations.

[12] We determine $K(z)$ by fitting the ^{40}Ar data assuming that the escape flux of ^{40}Ar is zero. This is reasonable because ^{40}Ar is relatively heavy and therefore far less abundant at the top of the atmosphere and in the exosphere than CH_4, H_2, or N_2. Assuming an exobase of 1500 km, the vertical column densities of N_2, CH_4, and ^{40}Ar in the exosphere are 3×10^{14}, 4×10^{13}, and 3×10^8 cm^{-2}, respectively. Thus, any escape processes that is species-independent should cause negligible ^{40}Ar escape. There are no known escape processes that would favor ^{40}Ar over other molecular species. The ^{40}Ar mole fraction at the lower boundary is fixed at 4.3×10^{-5}, the value determined from Cassini/GCMS measurements [*Niemann et al.*, 2005]. The GCMS measurements were made at a latitude of 8°S, whereas the INMS measurements cover a range of latitudes in Titan's northern hemisphere. However, ^{40}Ar should be homogeneously distributed throughout Titan's lower atmosphere because it is chemically inert, does not condense, and has no sources or sinks in the atmosphere.
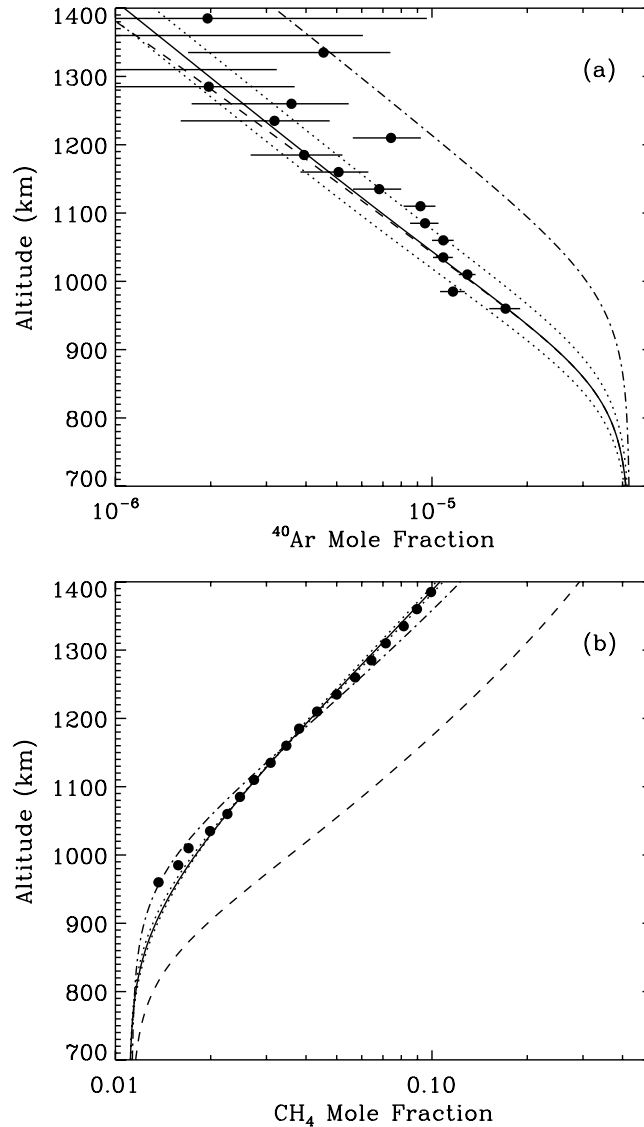
Figure 4. Mole fraction inferred from the data along with diffusion models for (a) CH_4 and (b) ^{40}Ar. The solid line represents model A, the dashed line is for model B, and the dot-dashed line represents model C. The dotted lines represent models D and E, with the larger ^{40}Ar mole fractions corresponding to the larger value of K_∞. CH_4 mole fractions for models D and E are indistinguishable from model A.

[13] We model the eddy profile with

$$K(z) = \frac{K_\circ(p_\circ/p)^\gamma K_\infty}{K_\circ(p_\circ/p)^\gamma + K_\infty} \quad (4)$$

where p is the pressure, $p_\circ = 1.43$ dyn cm^{-2}, $K_\circ = 3 \times 10^2$ cm^2 s^{-1} and $\gamma = 0.9$. This parameterization is chosen for consistency with photochemical models, which require a small value of $K(z)$ in the lower stratosphere to reproduce observed levels of photochemical species [*Vuitton et al.*, 2008]. The asymptotic value at high altitude, K_∞, is the only parameter that effects the distribution of ^{40}Ar and CH_4 in the altitude range considered here.

[14] Figure 4a shows the ^{40}Ar profiles for several models with different values of K_∞. Model parameters are summarized in Table 1. A value of $K_\infty = 3 \times 10^7$ cm^2 s^{-1} provides the best fit to the data while $K_\infty = 2 \times 10^7$ cm^2 s^{-1}
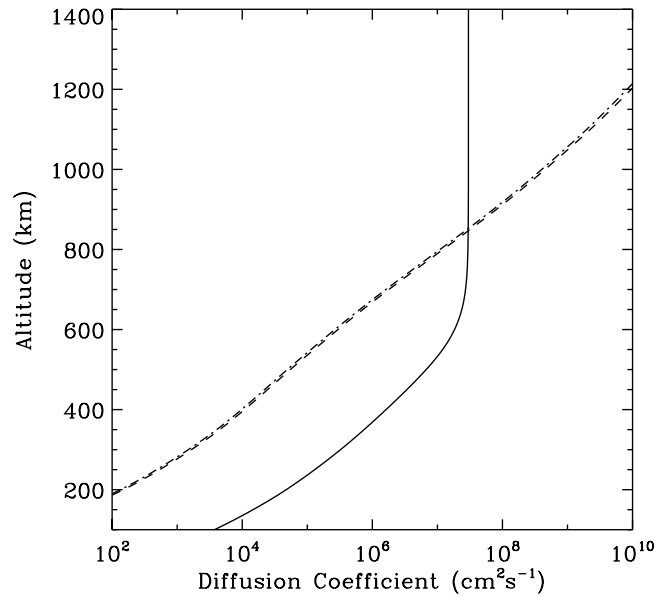
and $K_\infty = 5 \times 10^7$ cm^2 s^{-1} provide reasonable lower and upper limits. The eddy diffusion profile and molecular diffusion coefficient for ^{40}Ar are shown in Figure 5. Diffusive separation becomes important above $\sim$750 km and the homopause occurs at 850 km.

[15] A diffusive equilibrium model for CH_4, using $K(z)$ determined from the ^{40}Ar data, is compared with the observed CH_4 mole fraction in Figure 4b. This model predicts much larger mole fractions than inferred from the

Table 1. Model Parameters

Model	K_∞ (cm^2 s^{-1})	$F(CH_4)$ (cm^{-2} s^{-1})
A	3.0×10^7	2.8×10^9
B	3.0×10^7	0
C	4.0×10^8	0
D	2.0×10^7	3.0×10^9
E	5.0×10^7	2.5×10^9

Figure 5. The eddy diffusion profile adopted in this study along with the molecular diffusion coefficients for CH_4 (dashed line) and ^{40}Ar (dash-dotted line).

INMS measurements. The problem is that the observed mole fraction at 950 km is roughly equal to the value in the deep atmosphere of 1.4% inferred from GCMS measurements [*Niemann et al.*, 2005]. Thus, at 950 km, there has been very little diffusive separation of CH_4, whereas ^{40}Ar is well into the diffusive separation region. As shown in Figure 5, the ^{40}Ar and CH_4 molecular diffusion coefficients are quite similar and diffusive separation should occur in the same altitude region.

[16] The model can be brought into agreement with the data by postulating an upward flux of CH_4. As discussed in section 1, a large upward flux forestalls the onset of diffusive equilibrium and mimics the effects of eddy diffusion. The flux must be close to the limiting flux to be effective. The limiting flux for CH_4 is approximately 3.0×10^9 cm^{-2} s^{-1} and we find that the data is best fit by a CH_4 flux of $F(CH_4) = 2.8 \times 10^9$ cm^{-2} s^{-1}, referred to the surface. The lower and upper limits to the escape flux, correspond to the upper and lower limits to K_∞ and have values of 2.5×10^9 and 3.0×10^9 cm^{-2} s^{-1}.

[17] *Strobel et al.* [1992] determined an eddy coefficient for Titan's upper atmosphere of $4–8 \times 10^8$ cm^2 s^{-1} from analysis of CH_4 densities inferred from Voyager UVS measurements [*Smith et al.*, 1982; *Vervack et al.*, 2004]. We also show in Figure 4b a model with $K_\infty = 4 \times 10^8$ cm^2 s^{-1}. This model does provide an adequate fit to the CH_4 data, but, as shown in Figure 4a, it predicts an ^{40}Ar mole fraction a factor of ∼3 larger than observed at 1000 km. Thus, the atmospheric structure measured by Cassini is consistent with that found by Voyager, but the availability of the ^{40}Ar data completely changes the interpretation.

[18] The best fit to the INMS data has a CH_4 mole fraction in the deep atmosphere of 1.1%, which is 30% smaller than the value inferred from GCMS measurements [*Niemann et al.*, 2005]. The GCMS values pertains to the equatorial atmosphere and the INMS data to an average for the northern hemisphere. Latitudinal variations of CH_4

mole fraction in the stratosphere are one possible explanation for the difference; however, horizontal transport times in Titan's lower stratosphere are much faster than vertical diffusion times [*Hourdin et al.*, 2004] and a relatively inert constituent, such as CH_4 should be uniformly mixed. The difference might also be instrumental in origin. The sensitivity calibration of the INMS is roughly 20% [*Waite et al.*, 2004], of the same order as the disagreement. More troubling is the systematic departure of the model from the data at altitudes below 1000 km (Figure 4b). There may be several explanations for this. As discussed by *Yelle et al.* [2006] and *Müller-Wodarg et al.* [2008], the primary channels of the INMS used to determine the N_2 and CH_4 densities become saturated at these altitudes and data reduction becomes more complex. This could be responsible for systematic errors in the derived mole fractions. Alternatively, the disagreement may simply reflect the intrinsic inaccuracies of a 1D model. In any case, the disagreement between model and data is of order 20% while the effect of the CH_4 escape flux is a factor of ∼3; thus, these problems do not appear to affect our primary conclusions in a significant way, though they may affect numerical values at the level of ∼20%.

[19] The analysis presented here along with previous studies of diffusion on Titan have treated CH_4 as a inert constituent. This is permissible, even though CH_4 is destroyed by photochemistry, because the time constant for diffusion is much smaller than the time constant for photolysis. At 850 km the CH_4 diffusion coefficient is $D = 3 \times 10^7$ cm^2 s^{-1} and the scale height, $H = 92$ km. The diffusion time constant, given by $t_D = H^2/D$ is 3×10^6 s. The altitude region near 850 km is also where photolysis of CH_4 by solar H Lyα is a maximum. Adopting a solar Lyα flux at 1 AU of 4×10^{11} photons cm^{-2} s^{-1} and an absorption cross section of 2×10^{-17} cm^2 implies a photolysis time of 2×10^7 s, nearly an order of magnitude longer than the diffusion time. We note that inclusion of photolysis in our diffusion models would increase the

derived CH_4 flux slightly because photolysis would cause a decrease in CH_4 mole fraction with increasing altitude.

[20] Rigorously speaking, the CH_4 flux derived in our analysis is not necessarily an escape flux but rather the flux of CH_4 leaving the local atmosphere. Bearing in mind that the data and models represent an average for the northern hemisphere, to interpret the flux as something other than an escape flux requires postulating that the molecules leaving the northern hemisphere return to the southern hemisphere. As yet, we have little data on the upper atmosphere in Titan's southern hemisphere, but we consider the possibility of significant flow from the northern hemisphere to the southern hemisphere unlikely. Ballistic transport through the exosphere is not a possibility. The horizontal distance covered by an average ballistic trajectory is roughly twice the scale height or 200 km for CH_4, i.e., a small fraction of Titan's radius. Thus, thermal CH_4 molecules do not really leave the vicinity. Exceedingly large winds in the upper atmosphere that could carry CH_4 from the northern hemisphere to the southern hemisphere also seem improbable because it is currently southern summer on Titan and the available evidence on Titan suggests that the north polar region is the site of convergence rather than divergence [*Müller-Wodarg et al.*, 2008]. It is exceedingly unlikely that meridional winds could flow counter to the large latitudinal temperature gradient in Titan's upper atmosphere. Thus, the only reasonable explanation is that the upward flux of CH_4 represents an escape flux.

4. Discussion

[21] The eddy diffusion coefficient derived here is more similar to that found in other planetary atmospheres than were the large values derived in previous studies of Titan's upper atmosphere. The eddy diffusion coefficients on Venus and Mars are estimated to be 3×10^7 and 4×10^7 cm^2 s^{-1}, respectively [*Massie et al.*, 1983; *Krasnopolsky*, 1993], very similar to the value derived here. The eddy coefficient at the homopause on Jupiter is roughly 5×10^6 cm^2 s^{-1} [*Yelle et al.*, 1996] and the value for the Earth is 2×10^5 cm^2 s^{-1} [*Allen et al.*, 1981]. Thus, vertical mixing on Titan appears to be more similar to Venus and Mars than the Earth or Jupiter.

[22] The large CH_4 escape flux, if it persists over geological time scales, is likely to be marginally important in the evolution of the atmosphere. The H_2 escape rate on Titan is approximately 10^{10} m^{-2} s^{-1} [*Yelle et al.*, 2006], [*Cui et al.*, 2008] Assuming that the dominant chemical process in Titan's atmosphere is conversion of CH_4 to C_2H_6 [*Yung et al.*, 1984], each escaping H_2 molecule implies destruction of two CH_4 molecules. Thus, an H_2 escape flux of 10^{10} m^{-2} s^{-1} implies a CH_4 flux of 2×10^{10} m^{-2} s^{-1}, roughly a factor 7 larger than the CH_4 escape rate. Thus, CH_4 escape will shorten the lifetime of the atmosphere, but only a small factor.

[23] The existence of a large escape flux of CH_4 appears to be well established, but the escape mechanism is not clear. Jeans escape of CH_4 is insignificant. Using the temperatures and densities reported above, we estimate a Jeans escape flux of 0.5 cm^{-2} s^{-1}, i.e., essentially zero. Nonthermal escape mechanisms are also difficult to identify. The vertical column density of CH_4 in the exosphere is

approximately 4×10^{13} cm^{-2}. Thus, an escape flux of 2.8×10^9 m^{-2} s^{-1} requires a loss time of $\sim 10^{-4}$ s^{-1}. The photodestruction time for CH_4 is roughly 2×10^{-8} s^{-1}, many orders of magnitude too small. The ionization rate by energetic electrons in the magnetosphere is also insufficient. Adopting an energetic electron density of 0.1 cm^{-3}, a mean energy of 200 eV [*Hartle et al.*, 2006], and an ionization cross section of 3×10^{-16} cm^{-2} implies an ionization rate of 2×10^{-8} s^{-1}, similar to the photodestruction time and likewise far too small to explain the large escape flux.

[24] Assuming that each escaping molecule carries off an energy equal to the gravitational potential energy implies that the escaping energy is 1.6×10^{-3} ergs cm^{-2} s^{-1}, which is roughly 10% of the solar EUV energy absorbed in Titan's upper thermosphere. Thus, whatever escape mechanism is responsible must tap in to a reservoir of energy comparable to the thermal reservoir in the upper atmosphere. Recently, *Strobel* [2008], in response to preliminary presentations of the work described here, has suggested that thermal escape may proceed at a rate much greater than implied by the Jeans escape formula. The main point is that the escape process should be treated as hydrodynamic rather than stationary as with the Jeans approximation. A thorough investigation of this provocative suggestion along with comparison to the data presented here is needed but is outside the scope of this paper.

References

Allen, M., Y. L. Yung, and J. W. Waters (1981), Vertical transport and photochemistry in the terrestrial mesosphere and lower thermosphere 50–120 km, *J. Geophys. Res.*, 86, 3617–3627.

Cui, J., R. Yelle, and K. Volk (2008), Distribution and escape of molecular hydrogen in Titan's thermosphere and exosphere, *J. Geophys. Res.*, 113, E10004, doi:10.1029/2007JE003032.

Hartle, R. E., et al. (2006), Preliminary interpretation of Titan plasma interaction as observed by the Cassini Plasma Spectrometer: Comparisons with Voyager 1, *Geophys. Res. Lett.*, 33, L08201, doi:10.1029/2005GL024817.

Hourdin, F., S. Lebonnois, D. Luz, and P. Rannou (2004), Titan's stratospheric composition driven by condensation and dynamics, *J. Geophys. Res.*, 109, E12005, doi:10.1029/2004JE002282.

Hunten, D. M. (1973a), The escape of H_2 from Titan, *J. Atmos. Sci.*, 30, 726–732.

Hunten, D. M. (1973b), The escape of light gases from planetary atmospheres, *J. Atmos. Sci.*, 30, 1481–1494.

Krasnopolsky, V. A. (1993), Photochemistry of the Martian atmosphere (mean conditions), *Icarus*, 101, 313–332, doi:10.1006/icar.1993.1027.

Mason, E. A., and T. R. Marrero (1970), The diffusion of atoms and molecules, *Adv. At. Mol. Phys.*, 6, 155–232.

Massie, S. T., D. M. Hunten, and D. R. Sowell (1983), Day and night models of the Venus thermosphere, *J. Geophys. Res.*, 88, 3955–3969.

Müller-Wodarg, I. C. F., and R. V. Yelle (2002), The effect of dynamics on the composition of Titan's upper atmosphere, *Geophys. Res. Lett.*, 29(23), 2139, doi:10.1029/2002GL016100.

Müller-Wodarg, I. C. F., R. Yelle, J. Cui, and J. Waite (2008), Horizontal structures and dynamics of Titan's thermosphere, *J. Geophys. Res.*, 113, E10005, doi:10.1029/2007JE003033.

Niemann, H. B., et al. (2005), The abundances of constituents of Titan's atmosphere from the GCMS instrument on the Huygens probe, *Nature*, 438, 779–784.

Shemansky, D. E., A. I. F. Stewart, R. A. West, L. W. Esposito, J. T. Hallett, and X. Liu (2005), The Cassini UVIS stellar probe of the Titan atmosphere, *Science*, 308, 978–982, doi:10.1126/science.1111790.

Smith, G. R., D. F. Strobel, A. L. Broadfoot, B. R. Sandel, D. E. Shemansky, and J. B. Holberg (1982), Titan's upper atmosphere: Composition and temperature from the EUV solar occultation results, *J. Geophys. Res.*, 87, 1351–1359.

Strobel, D. F. (2008), Titan's hydrodynamically escaping atmosphere, *Icarus*, *193*, 588–594.

Strobel, D. F., M. E. Summers, and X. Zhu (1992), Titan's upper atmosphere—Structure and ultraviolet emissions, *Icarus*, *100*, 512–526, doi:10.1016/0019-1035(92)90114-M.

Vervack, R. J., B. R. Sandel, and D. F. Strobel (2004), New perspectives on Titan's upper atmosphere from a reanalysis of the Voyager 1 UVS solar occultations, *Icarus*, *170*, 91–112, doi:10.1016/j.icarus.2004.03.005.

Vinatier, S., B. Bézard, T. Fouchet, N. A. Teanby, R. de Kok, P. G. J. Irwin, B. J. Conrath, C. A. Nixon, P. N. Romani, F. M. Flasar, and A. Coustenis (2007), Vertical abundance profiles of hydrocarbons in Titan's atmosphere at 15°S and 80°N retrieved from Cassini/CIRS spectra, *Icarus*, *188*, 120–138, doi:10.1016/j.icarus.2006.10.031.

Vuitton, V., R. V. Yelle, and J. Cui (2008), Formation and distribution of benzene on Titan, *J. Geophys. Res.*, *113*, E05007, doi:10.1029/2007JE002997.

Waite, J. H., W. S. Lewis, W. T. Kasprzak, V. G. Anicich, B. P. Block, T. E. Cravens, G. G. Fletcher, W.-H. Ip, J. G. Luhmann, R. L. McNutt, H. B. Niemann, J. K. Parejko, J. E. Richards, R. L. Thorpe, E. M. Walter, and R. V. Yelle (2004), The Cassini Ion and Neutral Mass Spectrometer (INMS) Investigation, *Space Science Reviews*, *114*, 113–231, doi:10.1007/s11214-004-1408-2.

Waite, J. H., D. T. Young, T. E. Cravens, A. J. Coates, F. J. Crary, B. Magee, and J. Westlake (2007), The Process of Tholin Formation in Titan's Upper Atmosphere, *Science*, *316*, 870, doi:10.1126/science.1139727.

Yelle, R. V., L. A. Young, R. J. Vervack, R. Young, L. Pfister, and B. R. Sandel (1996), Structure of Jupiter's upper atmosphere: Predictions for Galileo, *J. Geophys. Res.*, *101*, 2149–2162.

Yelle, R. V., N. Borggren, V. de La Haye, W. T. Kasprzak, H. B. Niemann, I. Müller-Wodarg, and J. H. Waite (2006), The vertical structure of Titan's upper atmosphere from Cassini Ion Neutral Mass Spectrometer measurements, *Icarus*, *182*, 567–576, doi:10.1016/j.icarus.2005.10.029.

Yung, Y. L., M. Allen, and J. P. Pinto (1984), Photochemistry of the atmosphere of Titan—Comparison between model and observations, *Astrophys. J. (Supp.)*, *55*, 465–506, doi:10.1086/190963.

———————————

J. Cui and R. V. Yelle, Department of Planetary Sciences, University of Arizona, 1169 E. University Boulevard, Tucson, AZ 85721, USA. (jcui@lpl.arizona.edu; yelle@lpl.arizona.edu)

I. C. F. Müller-Wodarg, Space and Atmospheric Physics Group, Imperial College London, Prince Consort Road, London SW7 2BW, UK. (i.muellerwodarg@imperial.ac.uk)